

1 **RNA-seq analysis of early enteromyxosis in turbot (*Scophthalmus maximus*): new insights into**
2 **parasite invasion and immune evasion strategies**

3 Paolo Ronza ^{a,1}, Diego Robledo ^{b,1}, Roberto Bermúdez ^c, Ana Paula Losada ^a, Belén G. Pardo ^d,
4 Ariadna Sitjà-Bobadilla ^e, María Isabel Quiroga ^{a,*}, Paulino Martínez ^d

5 ^a*Departamento de Ciencias Clínicas Veterinarias, Facultad de Veterinaria, Universidade de*
6 *Santiago de Compostela, 27002 Lugo, Spain*

7 ^b*Departamento de Genética, Facultad de Biología (CIBUS), Universidade de Santiago de*
8 *Compostela, 15782 Santiago de Compostela, Spain*

9 ^c*Departamento de Anatomía y Producción Animal, Facultad de Veterinaria, Universidade de*
10 *Santiago de Compostela, 27002 Lugo, Spain*

11 ^d*Departamento de Genética, Facultad de Veterinaria, Universidade de Santiago de Compostela,*
12 *27002 Lugo, Spain*

13 ^e*Instituto de Acuicultura Torre de la Sal (IATS-CSIC), 12595 Ribera de Cabanes, Castellón, Spain*

14 ¹Authors contributed equally to this article.

15

16 *Corresponding author: María Isabel Quiroga, Departamento de Ciencias Clínicas Veterinarias,
17 Facultad de Veterinaria, Universidade de Santiago de Compostela, 27002 Lugo, Spain.
18 Tel.: +34 982822304; fax: +34 982252195.

19

20 E-mail address: misabel.quiroga@usc.es

21

22 This is an Accepted Manuscript of an article published by Elsevier in Gene, available online: <https://doi.org/10.1016/j.gene.2011.10.020>.

23 © 2011 Elsevier B.V. This is an open access article under the CC BY-NC-ND license
<http://creativecommons.org/licenses/by-nc-nd/4.0/>

24

25

26

27 **Abstract**

28 *Enteromyxum scophthalmi*, an intestinal myxozoan parasite, is the causative agent of a
29 threatening disease for turbot (*Scophthalmus maximus*, L.) aquaculture. The colonization of the
30 digestive tract by this parasite leads to a cachectic syndrome associated with high morbidity and
31 mortality rates. This myxosporidiosis has a long pre-patent period and the first detectable clinical
32 and histopathological changes are subtle. The pathogenic mechanisms acting in the early stages of
33 infection are still far from being fully understood. Further information on the host-parasite
34 interaction is needed to assist in finding efficient preventive and therapeutic measures. Here, a
35 RNA-seq-based transcriptome analysis of head kidney, spleen and pyloric caeca from
36 experimentally-infected and control turbot was performed. Only infected fish with early signs of
37 infection, determined by histopathology and immunohistochemical detection of *E. scophthalmi*,
38 were selected. The RNA-seq analysis revealed, as expected, less intense transcriptomic changes
39 than those previously found during later stages of the disease. Several genes involved in IFN-related
40 pathways were up-regulated in the three organs, suggesting that the IFN-mediated immune response
41 plays a main role in this phase of the disease. Interestingly, an opposite expression pattern had been
42 found in a previous study on severely infected turbot. In addition, possible strategies for immune
43 system evasion were suggested by the down-regulation of different genes encoding complement
44 components and acute phase proteins. At the site of infection (pyloric caeca), modulation of genes
45 related to different structural proteins was detected and the expression profile indicated the
46 inhibition of cell proliferation and differentiation. These transcriptomic changes provide indications
47 regarding the mechanisms of parasite attachment to and invasion of the host. The current results
48 contribute to a better knowledge of the events that characterize the early stages of turbot
49 enteromyxosis and provide valuable information to identify molecular markers for early detection
50 and control of this important parasitosis.

51 **Keywords:** RNA-seq, Transcriptome, Turbot, *Enteromyxum scophthalmi*, Myxozoa, Pathogenesis

52 **1. Introduction**

53 Turbot (*Scophthalmus maximus*, L.) is a valuable cultured marine flatfish, whose production
54 in 2013 accounted for over 77,000 tons, with China (67,000 tons in 2013) and the European Union
55 (7,700 tons in 2013, 11,000 in 2014) as the main producers (APROMAR, 2015). Enteromyxosis
56 caused by *Enteromyxum scophthalmi* (Myxozoa) is a serious threat for turbot aquaculture, currently
57 without effective therapeutic measures (Sitjà-Bobadilla and Palenzuela, 2012). The target site of
58 this myxozoan parasite is the gastrointestinal tract, where it proliferates and spreads from the
59 anterior intestine and pyloric caeca to other gut regions (Redondo et al., 2004). The infection leads
60 to severe catarrhal gastroenteritis associated with a cachectic syndrome, with reduction of growth
61 performance and high mortality rates (Bermúdez et al., 2010; Sitjà-Bobadilla and Palenzuela, 2012).
62 Under culture conditions, the trophozoites are transmitted directly from fish to fish, which leads to a
63 rapid spread of disease in infected tanks and facilities (Redondo et al., 2002; Quiroga et al., 2006;
64 Sitjà-Bobadilla and Palenzuela, 2012). However, the disease shows a long pre-patent period, with
65 the parasite detectable in the digestive tract by histology only after several weeks in natural
66 infections (Redondo et al., 2004; Quiroga et al., 2006). In experimental infections by effluent
67 transmission or cohabitation, the parasite is first observed at approximately 20 days post-exposure,
68 and at approximately 8 days after experimental per os transmission (Redondo et al., 2004;
69 Bermúdez et al., 2006; Sitjà-Bobadilla et al., 2006; Losada et al., 2014a). Experimental infection by
70 the oral route results in a very high and quick prevalence of infection and homogeneous lesions in
71 recipient fish. In addition, the ingestion of trophozoites released from infected fish is thought to be
72 the main infection route occurring in the fish farm (Redondo et al., 2002, 2004). In the early stages
73 of infection there are no external clinical signs, histological lesions are very subtle, and the parasite
74 is difficult to detect in conventional histological sections of the digestive tract (Quiroga et al., 2006;
75 Bermúdez et al., 2010). In vitro, *E. scophthalmi* is able to penetrate the intestinal epithelium from
76 the lumen as well as via the basement membrane, and the report of parasitic stages in blood smears

77 suggests the existence of a haematic route of spread (Redondo et al., 2003, 2004; Redondo and
78 Álvarez-Pellitero, 2010). However, a detailed understanding of entry routes and epithelial invasion
79 strategies is lacking. We are still far from a full knowledge of the host-parasite interaction and
80 further investigation is needed to clarify the pathogenetic mechanisms of enteromyxosis (Sitjà-
81 Bobadilla and Palenzuela, 2012; Robledo et al., 2014), especially those acting during early stages of
82 infection.

83 Whole-transcriptome analysis using RNA-seq is a suitable approach for the identification of
84 the genes and pathways involved in host-pathogen interactions, and it is acquiring a key role in the
85 understanding of the pathogenesis of human and veterinary diseases (Costa et al., 2013; Qian et al.,
86 2014; Li et al., 2015). This is an essential starting point for the development of control measures,
87 therapeutic options and genetic breeding programs. An RNA-seq analysis of turbot experimentally
88 infected by the oral route was previously addressed, investigating the advanced stages of the disease
89 by studying specimens at 42 days post-inoculation. That work enabled a better understanding of the
90 genetic basis of the clinical signs and lesions which characterize the infection (Robledo et al.,
91 2014). In this study, using a similar methodological approach, we performed a transcriptomic
92 analysis of turbot showing very early signs of infection aimed at contributing to the current
93 understanding of incipient enteromyxosis.

94

95 **2. Materials and methods**

96 *2.1. Experimental design*

97 The experimental setup and sampling were as previously described (Robledo et al., 2014).
98 Briefly, infection was achieved by the oral route (Redondo et al., 2002) and tissue samples were
99 collected in Bouin's fluid and RNAlater (Qiagen, Germany) for histological techniques and RNA-
100 seq, respectively. A histological evaluation was performed, and infected turbot were classified into

101 three groups (slightly, moderately and severely infected) according to the histopathological grading
102 described by Bermúdez et al. (2010). For RNA-seq analysis, spleen, head kidney and pyloric caeca
103 from three control (CTRL) and three *E. scophthalmi*-infected (recipient, RCPT) fish at 24 days
104 post-inoculation were used. The three RCPT fish were selected by histology among those graded as
105 slightly infected and numbered (infected turbot 1, 2 and 3). RNA aliquots from the samples of
106 RCPT fish were sequenced individually, while samples from CTRL fish were pooled by organ,
107 resulting in three RCPT and one CTRL sample per organ.

108

109 2.2. Immunohistochemistry

110 Immunohistochemical detection of *E. scophthalmi* was performed on sections from different
111 regions of the digestive tract (oesophagus, stomach, pyloric caeca, anterior, middle and posterior
112 intestine) to confirm the presence of the parasite. Thin sections (3 µm) were placed on slides treated
113 with silane to improve section adherence and dried overnight at 37 °C. After deparaffination (two 5
114 min washes in xylene) and rehydration (graded alcohol series), the endogenous peroxidase activity
115 was inhibited by incubating the slides with peroxidase-blocking solution (Dako, Denmark) for 40
116 min. A 2 h incubation at room temperature was performed with a polyclonal antibody against *E.*
117 *scophthalmi* (Estensoro et al., 2014) (diluted 1: 50,000). The secondary antibody conjugated with
118 peroxidase was the anti-rabbit EnVision+ System Labelled Polymer-HRP (Dako) for 30 min,
119 followed by development with diaminobenzidine (Dako). All incubations were performed in humid
120 chambers and three 5 min washes with 0.01 M PBS were carried out between all subsequent steps.
121 Sections of severely infected turbot were used as positive controls. In the sections included as
122 negative controls, the primary antibody was replaced by antibody diluents.

123

124 2.3. RNA-seq and differential expression analysis

125 Some of the procedures and methodologies employed were described previously (Robledo et
126 al., 2014). Briefly, RNA extraction was performed using the RNeasy mini kit (Qiagen, Germany)
127 with DNase treatment and RNA quality and quantity were evaluated in a Bioanalyzer (Bonsai
128 Technologies, Spain) and in a NanoDrop® ND-1000 spectrophotometer (NanoDrop® Technologies
129 Inc., Delaware, US), respectively. The samples were barcoded and prepared for sequencing by the
130 Wellcome Trust Centre for Human Genetics (Oxford, UK) and sequenced on an Illumina HiSeq
131 2000 as 100 bp paired-end reads. All the data files have been deposited in the National Center for
132 Biotechnology Information (NCBI) Short Read Archive (SRA) database under the project ID
133 PRJNA300347; as well the generated transcriptome sequences and their annotation have been
134 deposited in Mendeley Data (<https://data.mendeley.com/>) and can be accessed using doi:
135 10.17632/3vhc8py3cv.2. Quality filtering and removal of residual adaptor sequences was conducted
136 using Trimmomatic v.0.32 (Bolger et al., 2014). The recently assembled turbot genome (Figueras et
137 al., 2016) was used as a reference for read mapping. Filtered reads were mapped to the genome
138 using Tophat2 v.2.0.11 (Kim et al., 2013) which leverages the short read aligner Bowtie2 v.2.2.3
139 (Langmead and Salzberg, 2012) with a maximum intron length of 20 kb. HTSeq-count
140 (<http://www-huber.embl.de/users/anders/HTSeq/doc/overview.html>) was used to extract the raw
141 reads from the mapping files and differentially expressed genes were obtained using EdgeR
142 (Robinson and Oshlack, 2010) with a False Discovery Rate (FDR) corrected *P* value of 0.05. The
143 differentially expressed (DE) genes were identified and annotated using Blast2GO v.2.7.0 (Conesa
144 et al., 2005) with an E-value cutoff of E^{-6} . Enriched Gene Ontology (GO) terms for each organ were
145 identified by comparing the DE genes against the full transcriptome using Blast2GO Fisher's exact
146 test ($P < 0.05$, FDR corrected). Furthermore, in this study, Kyoto Encyclopedia of Genes and
147 Genomes (KEGG, Kanehisa et al., 2016)) enrichment was assessed using KOBAS 2.0 (Wu et al.,
148 2006) ($P < 0.05$, FDR corrected) with the draft turbot genome annotation as background. Those
149 reads from pyloric caeca samples which did not align against the genome, both from turbot of this
150 study (at 24 days post-inoculation) and from a previous study with parasitized turbot at 42 days

151 post-inoculation (Robledo et al. 2014), were extracted and de novo transcriptome assembly was
152 carried out using ABySS (version 1.3.7; Simpson et al., 2009) with a 64 k-mer size, scaffolding and
153 contig options on, and remaining parameters set to default values. Expression values were
154 individually estimated for each pyloric caeca sample by counting reads for each transcript after
155 aligning the genome-unaligned reads of the sample against the reconstructed de novo transcriptome
156 using RSEM v.1.2.17 (Li and Dewey, 2011). Differential expression between infected and control
157 groups was estimated using EdgeR (FDR corrected P value < 0.05 ; Robinson and Oshlack, 2010).

158

159 **3. Results and discussion**

160 *3.1. Histopathology revealed minor tissue alterations and the presence of E. scophthalmi*

161 The histological evaluation of RCPT turbot revealed minor alterations at an intestinal level.
162 Slight inflammatory infiltrates, mostly composed of mononuclear cells, were occasionally detected
163 in the lamina propria-submucosa or at the base of the epithelial lining of pyloric caeca and anterior
164 intestine (Fig. 1A, B, D). In these areas, basophilic structures consistent with early stages of the
165 parasite were observed (Fig. 1A, B). The specimen labelled as "infected turbot 2" also presented
166 some trophozoites in the hindgut, and was the only fish which sporadically showed more advanced
167 developmental stages of *E. scophthalmi*, stages 2 or 3 according to Redondo et al. (2004) (Figs. 1D,
168 E). The histological features of the three RCPT fish were in accordance with the "slight infection"
169 degree described by Bermúdez et al. (2010). No significant changes were detected in the remaining
170 examined organs, nor in CTRL fish. The presence of parasitic stages was then confirmed by
171 immunohistochemistry (Fig. 1C, F), supporting the histological observations.

172

173 *3.2. Pyloric caeca showed higher percentages of unaligned reads*

174 A total of ~170 million 100 bp pair-end reads were sequenced, the same amount as in the
175 previous work with severely infected turbot, accounting on average for 13.3 million reads post-
176 filtering per sample, slightly below the 15 million reads per sample formerly obtained (Robledo et
177 al., 2014). A total of 138 million (86.5%) of the filtered reads (~160 million) were mapped to the
178 turbot genome. A notable difference was found between this and the previous study when
179 comparing the result of the alignments for pyloric caeca. In slightly infected turbot, 90% of the
180 trimmed reads aligned to the genome, while in severely infected turbot only 65% aligned (Robledo
181 et al., 2014). The unaligned reads of both 24 and 42 days post-inoculation samples from pyloric
182 caeca were used to reconstruct a de novo transcriptome (a brief comparison between genome-
183 guided and de novo assemblies is shown in Table 1), and differential expression analysis between
184 infected and control samples was carried out. No sequences annotated to *Enteromyxum* spp. were
185 detected among DE genes at 24 days post-inoculation, but six transcripts, annotated as *E.*
186 *scophthalmi* 18S subunit ribosomal gene, and two more as *Enteromyxum leei* 28s subunit ribosomal
187 gene, were found DE at 42 days post-inoculation. The fact that no DE *Enteromyxum* sequences
188 were found during early stages of the disease suggests that the concentration of the parasite in
189 pyloric caeca at that stage is low. On the other hand, another 422 up-regulated sequences were
190 found in pyloric caeca samples at 42 days post-inoculation, showing zero or one read in the control,
191 and annotated to invertebrate, plant, bacteria or fungi sequences (Supplementary Table S1). Some
192 of these sequences may correspond to new *Enteromyxum* sequences and constitute a resource for
193 exploration of host-parasite interactions in future studies, while others, especially those annotated to
194 bacteria, might reflect gut microbiota alterations caused by the disease.

195

196 3.3. Transcriptomic changes are subtle at early stages of infection

197 The aligned reads resulted in a total of 56,321 transcripts from 36,356 genes. Samples were
198 hierarchically clustered for each organ according to their transcript expression (Fig. 2). Samples

199 corresponding to the infected turbot 2 always clustered closest to the control samples, suggesting a
200 less intense response to infection. This is a remarkable result considering that this was the specimen
201 presenting more advanced stages of *E. scophthalmi* and more widespread and might suggest
202 silencing of the host response during some stages of the infection and/or an interindividual response
203 variation. On the other hand, infected turbot 1 and 3 constituted a different cluster only in pyloric
204 caeca, likely related to the stronger effect of the infection in this organ.

205 A total of 287, 211 and 187 DE genes were detected in head kidney, spleen and pyloric
206 caeca, highlighting the huge transcriptomic changes between the early and the advanced stage of the
207 disease, where the numbers were 1,316, 1,377 and 3,022, respectively (Robledo et al., 2014). As
208 previously described (Robledo et al., 2014), relevant DE genes were grouped in five key broad
209 functional categories: immune and defence response, apoptosis and cell proliferation, cytoskeleton
210 and extracellular matrix, iron metabolism and erythropoiesis, and metabolism and digestive
211 function. Yet, in this study, DE genes related to cell differentiation were included in the category
212 “apoptosis and cell proliferation”, being renamed as “apoptosis, cell proliferation and
213 differentiation” (Supplementary Tables S2 - S4). Heatmaps of selected DE genes (Fig. 3), over-
214 represented GO terms (Fig. 4) and Venn diagrams comparing the total number of DE genes in the
215 early and advanced stages (24 and 42 days post-inoculation, Fig. 5 and Supplementary Table S5 –
216 S7) are presented.

217

218 *3.4. Immune and defence response: possible strategies for immune evasion and activation of* 219 *interferon-related pathways*

220 Some mechanisms of innate immunity were active during both early and late stages of the
221 disease (Robledo et al., 2014), such as the up-regulation in kidney and spleen of *ALOXE3* (full
222 gene names are shown in Supplementary Tables S2 - S4), acting on the metabolism of leukotrienes,

223 and *IL4I*, which participates in antigen processing. Also, *CD209*, a C-type lectin considered a
224 marker of antigen-presenting cells, was up-regulated in pyloric caeca as in the previous study,
225 adding new evidence about the role of this molecule in recognizing *E. scophthalmi*. In spleen, up-
226 regulation of genes related to endothelin, a vasoconstrictor peptide and chemoattractant of
227 macrophages, was also found in both studies. In early enteromyxosis, other up-regulated genes
228 acting in innate immunity were *CIQTNF9* and *GFIB* in spleen and pyloric caeca (Supplementary
229 Tables S3, S4), involved in inflammatory response, and *CCL19* in head kidney (Supplementary
230 Tables S2), a chemokine with chemotactic properties on lymphocytes and dendritic cells. On the
231 other hand, up-regulated genes associated with inhibition of the immune response were also
232 detected, such as *ZNFXI* in kidney and pyloric caeca, the transcription factor *FOXJ1* in pyloric
233 caeca and spleen, and *FOXJ1B* only in pyloric caeca. In the latter organ, these genes were related to
234 the over-represented GO terms associated with negative regulation of immune-related processes
235 (Fig. 4).

236 Some complement-related genes were down-regulated in the three organs. The most
237 remarkable result was detected in spleen, where the KEGG pathway “complement and coagulation
238 cascades” was enriched due to the down-regulation of several genes that constitute it
239 (Supplementary Fig. S1). Many products of these genes are considered acute phase proteins (APP),
240 such as the same complement components and different antiproteases. Also, other APP genes such
241 as haptoglobin, transferrin and ceruloplasmin, related to iron metabolism and antioxidant capacity,
242 were down-regulated in spleen. The acute phase response is an evolutionarily conserved immune
243 mechanism activated in teleosts by several infective agents including parasites (Bayne and Gerwick,
244 2001; Gerwick et al., 2002; Peatman et al., 2007; Khoo et al., 2012; Kovacevic et al., 2015). By
245 contrast, in the current parasite model, the opposite pattern was detected. This may reflect a
246 parasite-induced down-regulation as a strategy for immune system evasion or may be a temporary
247 exhaustion of this pathway following a previous activation. The first hypothesis would agree with

248 the pathogens targeting the complement system and host antiproteases as immune evasion strategies
249 (Armstrong, 2006; Zipfel et al., 2007), as well as with mechanisms for iron acquisition from host
250 cells (Ben-Othman et al., 2014; Leon-Sicairos et al., 2015). The second hypothesis would be in
251 accordance with previous observations in turbot exposed to *E. scophthalmi* by cohabitation (a
252 slower infection model), where serum complement activity by the alternative pathway was slightly
253 increased in infected fish at 20 days post-exposure but later (40 days post-exposure) decreased in
254 comparison with naïve fish (Sitjà-Bobadilla et al., 2006). Since the liver is the main producer of
255 complement components and APP, a time series study of the hepatic gene expression profile would
256 help to clarify this response during enteromyxosis.

257 Another result that strongly characterized this functional category was the up-regulation of
258 several genes related to the IFN-mediated immune response. The *PML* gene, which positively
259 regulates the type I IFN response by promoting transcription of IFN-stimulated genes (ISGs) (Kim
260 and Ahn, 2015), was up-regulated in the three organs. Head kidney showed the highest number of
261 DE genes related to IFN signalling, with an increased expression of IFN- γ , and sharing up-
262 regulation of IFN-induced Mx protein, *HERC4/5* and *IFIT1* with pyloric caeca and of *IFI44* and
263 IFN-inducible protein *gig2* with spleen. All in all, these results point towards a response mediated
264 by both type I and II IFNs, as observed in early stages of several mammalian protozoan infections
265 (Beiting, 2014). Also, the IFN-mediated immune response was shown to play a major role in
266 teleosts parasitized by amoebae and myxozoan parasites, with implications in fish resistance or
267 susceptibility to the disease (Young et al., 2008; Davey et al., 2011; Bjork et al., 2014). During
268 advanced stages of turbot enteromyxosis, IFN-related genes were markedly down-regulated in the
269 same organs, possibly indicating an association between the exhaustion of the IFN-mediated
270 response and the high susceptibility of turbot to enteromyxosis (Robledo et al., 2014). On the other
271 hand, this opposite pattern may also suggest that the immune response to *E. scophthalmi* is elicited

272 differently during the two stages of infection, perhaps depending on a change in the localization of
273 the parasite during the infection.

274 In this sense, the up-regulation of *STING* (also called *MITA*), *DHX58* and *TRIM25* observed
275 in head kidney and *MFNI* in pyloric caeca suggests activation of the RIG-I-like receptors (RLRs)
276 pathway. This pathway triggers the innate immune response against intracellular pathogens,
277 promoting the production of type I IFNs, ISGs and proinflammatory cytokines (Dixit and Kagan,
278 2013). RLR activation involves the participation of mitochondria, signalled through the
279 mitochondrial antiviral signalling protein (MAVS, also called IPS1) (Castanier et al., 2010;
280 Koshiba, 2013). *MFNI* mediates mitochondria fusion and encodes for a protein associated with
281 MAVS on the outer membrane of mitochondria, both being necessary for signal transduction in the
282 RLR pathway through the regulation of mitochondria dynamics (Castanier et al., 2010; Onoguchi et
283 al., 2010). This pathway is mainly known for viral recognition, but some evidence is emerging for
284 type I IFN production promoted by parasite-activated RLRs (Melo et al., 2013; Beiting, 2014).
285 Little is known about the pre-patent phase of enteromyxosis, but intracellular parasitic stages have
286 been described sporadically (Redondo et al., 2003, 2004; Quiroga et al., 2006), so it may be
287 hypothesized that an intracellular phase occurs during *E. scophthalmi* infection where the parasite is
288 recognized by RLRs. Head kidney also showed increased expression of *TRIM21*, described as an
289 intracellular antibody receptor and regulator of IFN pathways acting in viral infections (McEwan et
290 al., 2013; Vaysburd et al., 2013; Manocha et al., 2014), and of *SOCS1*, which plays an
291 evolutionarily conserved inhibitory role in the IFN signalling pathway (Nie et al., 2014). The
292 number of DE genes classically involved in antiviral defence showed by kidney is reflected by the
293 corresponding enriched GO term found, together with other immune-related categories (Fig. 4).
294 Both types of IFNs are also related to antigen presentation to cytotoxic cells via the major
295 histocompatibility complex class I (MHC-I) in teleosts (Zou and Secombes, 2011). In head kidney,
296 we found up-regulation of *HSP70* and *HSP90*, which participate in antigen presentation via the

297 MHC-I pathway, as do calreticulin and the MHC-I genes, whose expression was significantly
298 increased in one of the three infected fish (data not shown). The activation of natural killer (NK)
299 and cytotoxic T-cells was reflected by the up-regulation of *GZMA* in kidney and spleen, and *PRFI*
300 in kidney, both coding for cytolytic proteins found in granules of these cell types. MHC-I and T-
301 cells-related genes also showed an opposite expression pattern in the lymphohaematopoietic organs
302 of turbot with advanced enteromyxosis (Robledo et al., 2014).

303 In pyloric caeca, two up-regulated genes related to T-cells were detected, *LRRC32*, a
304 regulatory T (T-reg) specific receptor (Tran et al., 2009), and *NFIL3*, a transcription factor with
305 several important roles in the immune response, such NK cell function development, IL-3
306 transcription in T-cells and regulation of the Th2 cell response (Zhang et al., 1995; Kashiwada et
307 al., 2011). On the other hand, the gene for the T-cell surface antigen CD2 was down-regulated in
308 kidney and pyloric caeca. This molecule is present on T and NK cells, where it plays a role in cell
309 adhesion and acts as a co-stimulatory molecule for these cells. Decreased expression of *CD2* has
310 been found to be associated with infection by *Leishmania donovani* in human, causing impaired
311 CD4⁺ T-cell function and protective IFN- γ production (Bimal et al., 2008).

312 With regard to adaptive immunity, *RAG1*, a key gene for rearrangement and recombination
313 of immunoglobulin and T-cell receptor molecules during the VDJ recombination process, was up-
314 regulated in spleen. Nonetheless, little evidence was found for the activation of B cells, in
315 accordance with previous observations of a delayed humoral response (Bermúdez et al., 2006; Sitjà-
316 Bobadilla et al., 2006). Only pyloric caeca showed up-regulation of *PAX5*, a transcription factor
317 with a major role in B cells differentiation, and of the immunoglobulin-related gene Ig heavy chain
318 Mem5. Other interesting up-regulated genes in pyloric caeca, the target organ of the parasite, were
319 *RAC1*, a member of the small GTPase family, and *ACK1*, a downstream effector of another member
320 of this family, *CDC42*. These genes act in the c-Jun N-terminal protein kinases (JNK) pathway and
321 are involved in actin cytoskeleton remodelling induced by extracellular signals (Chen et al., 2004).

322 They have been implicated in host cell invasion by different pathogens including protozoan
323 parasites (Gruenheid and Finlay, 2003; Chen et al., 2004; Lodge and Descoteaux, 2006).

324

325 *3.5. Cytoskeleton and extracellular matrix: unravelling mechanisms of parasite attachment and*
326 *invasion*

327 Different genes encoding for components of the intracellular cytoskeleton (e.g. *FLNC*,
328 *SYNM* and *SYNPO2*) were down-regulated in pyloric caeca, suggesting parasite-induced
329 cytoskeleton remodelling of intestinal cells. Host cytoskeleton is a recognized early target of several
330 pathogens that infect epithelia for invasion of the host (Gruenheid and Finlay, 2003; Xu et al., 2008;
331 Radhakrishnan and Splitter, 2012), a mechanism also observed in teleost skin, gill and digestive
332 tract (Li et al., 2012, 2013; Sun et al., 2012). Another interesting adjustment in pyloric caeca was
333 the up-regulation of genes encoding for extracellular matrix (ECM) components such as *COL1A1*,
334 *TNN* and *FREMI*. The expression changes in genes related to ECM proteins may be difficult to
335 interpret because they might reflect either an early attempt at tissue repair by the host or the
336 pathogen manipulation and infection (Li et al., 2013). In fact, ECM proteins are often targeted by
337 many invasive pathogens, including parasites, for adhesion to and invasion of the host (Mittal et al.,
338 2008; Nde et al., 2012; Singh et al., 2012). Interestingly, *FREMI* has been recently postulated as a
339 novel candidate gene involved in human immunodeficiency virus (HIV) infection (Luo et al., 2012).
340 *Enteromyxum scophthalmi* is capable of attaching to and penetrating the intestinal epithelium, both
341 from the surface and the basal part, as shown by in vitro studies with intestinal explants (Redondo et
342 al., 2004; Redondo and Álvarez-Pellitero, 2010). In addition, in different experimental infections it
343 was observed that a longer time is needed to detect the parasite in intestinal histological sections
344 than in blood smears, blood being a hypothesized dispersion route (Redondo et al., 2003, 2004).
345 Hence, the possibility of epithelial invasion through the lamina propria-submucosa, involving an
346 interaction with ECM proteins, cannot be ruled out. Finally, a group of up-regulated DE genes in

347 this location were related to cell-cell junctions, in particular three genes encoding for claudins
348 (*CLDN10*, *CLDN14* and *CLDN18*), tight junction proteins, and for the adhesion protein *CDH26*.
349 These results are in accordance with the increasing expression trend found by real-time PCR for E-
350 cadherin (*CDH1*) in turbot with incipient infection (unpublished data). The junctional complexes
351 are essential to maintain the homeostasis of the intestinal barrier (Suzuki, 2013; Peterson and Artis,
352 2014) and this expression profile may be indicative of early repair mechanisms in response to the
353 parasite invasion of the lining epithelium. In advanced infection, it is plausible that the extension of
354 lesions, the severe inflammation and the prolonged fasting suffered by fish (Bermúdez et al., 2010;
355 Robledo et al., 2014) hinder an efficient activation and functioning of tissue repair at an intestinal
356 level.

357

358 3.6. Apoptosis, cell proliferation and differentiation: effects of *E. scophthalmi* on intestinal renewal

359 In addition to epithelial integrity, the constant renewal of the epithelium is a main defence
360 mechanism of the intestine against pathogens, and consequently a target for microbial
361 circumvention strategies (Kim et al., 2010). Accelerating the epithelial turnover has been described
362 as a host mechanism for parasite expulsion (Cliffe et al., 2005; Cortes et al., 2015), but several
363 mucosal pathogens can put in place stratagems to prevent their removal and successfully colonize
364 the lining epithelium (Iwai et al., 2007; Mimuro et al., 2007). In pyloric caeca of *E. scophthalmi*-
365 infected fish, there was a remarkable down-regulation of numerous genes related to cell
366 proliferation (e.g. *CCNB1*, *TPX2* and *CDC14A*) and differentiation (e.g. *HOXA9*, *HOXA10*, *VSIG1*).
367 Furthermore, *APC* and *TLX1*, which by contrast act as repressors of cell proliferation and
368 differentiation, showed an increased expression. Also *CASP3*, involved in apoptosis, was down-
369 regulated, unlike that observed in severely-infected turbot, which presented up-regulation of this
370 and other pro-apoptotic genes (Robledo et al., 2014). A biphasic modulation of apoptotic pathways,
371 consisting of early inhibition and late moderate promotion, was documented in human infection by

372 the intestinal parasite *Cryptosporidium parvum* (Liu et al., 2009). All in all, DE genes of this
373 functional category suggest that inhibitory mechanisms of epithelial renewal occur during incipient
374 enteromyxosis, which may facilitate the parasite's entrance and colonization of the digestive tract.
375 At later infection stages, the pathological changes observed in the intestinal epithelium, including
376 the increased apoptotic rate and enterocyte detachment, may be invoked by the exacerbated local
377 immune response (Bermúdez et al., 2010; Losada et al., 2012, 2014a; Robledo et al., 2014) and/or
378 induced by the parasite as a spreading strategy (Bermúdez et al., 2010). The only up-regulated gene
379 promoting cell proliferation was *CTGF*, a major connective tissue chemoattractant also involved in
380 ECM secretion, a finding in accordance with the aforementioned up-regulation of different ECM-
381 related genes.

382

383 3.7. Iron metabolism and erythropoiesis

384 Several genes related to haemoglobin (*HBB2* and *HBAD*), iron homeostasis and heme
385 biosynthesis (*FAM123B*; *SLC25A37* and *ALAS2*), and erythrocyte maturation and differentiation
386 (*GATA2* and *TALI*) showed an increased expression in pyloric caeca. Genes related to erythrocyte
387 structural (*DMTN*, *ANK1* and *RHAG*) and enzymatic (*CA*) components were also up-regulated.
388 These findings point towards an increased presence of red blood cells in the intestine of infected
389 turbot, consistent with hyperaemia. Hyperaemia is one of the first vascular changes which occur
390 after an inflammatory stimulus (McGavin and Zachary, 2006), a scenario consistent with early
391 infection of the digestive tract. On the other hand, a gene related to hepcidin (*HEP-2*), a main
392 regulator of iron metabolism, was down-regulated. In turbot, the existence of two hepcidin genes
393 has been reported (*HEP-1* and *HEP-2*), both showing antimicrobial properties and modulated
394 expression in response to bacterial and viral challenges (Pereiro et al., 2012; Zhang et al., 2014).
395 Nevertheless, a major role for *HEP-1* in body iron homeostasis has been previously suggested,
396 given that *HEP-2* expression did not change in liver in response to iron overload (Pereiro et al.,

397 2012). In our case, the down-regulation of *HEP-2* in pyloric caeca may be related to the
398 requirement of iron for heme biosynthesis, a hypothesis also supported by the contemporary up-
399 regulation of *FAMI23B*. The product of this gene is known as erythroferrone, an iron-regulatory
400 hormone with a potent suppressor action on hepcidin mRNA expression in mice (Kautz et al.,
401 2014). Under the hypotheses of a main role for *HEP-2* in innate immune response and considering
402 the expression profile of APP-related genes in the spleen, its down-regulation should also be
403 interpreted in the context of a global modulation of the immune response. Further research is
404 needed to clarify the role of APP and iron metabolism regulation during infection by *E.*
405 *scophthalmi*.

406

407 3.8. Metabolism and digestive function: diminished feeding activity

408 DE genes involved in digestive function were mostly down-regulated, including *VIP*,
409 *NPY2R* and *APOA4*. The only exception was the up-regulation of *GCG2*, a paralog of the glucagon
410 gene, which promotes hydrolysis of glycogen and lipids, thus increasing blood sugar levels (Moon,
411 1998). In previous immunohistochemical studies on the digestive tract of turbot with advanced
412 enteromyxosis, both VIP- and glucagon-immunoreactive cells showed decreases (Bermúdez et al.,
413 2007; Losada et al., 2014b). Also, *APOA4*, involved in lipids metabolism, was down-regulated in
414 the pyloric caeca of severely infected turbot analyzed by RNA-Seq (Robledo et al., 2014). The
415 down-regulation of a receptor of neuropeptide Y (*NPY2R*), a main regulator of appetite which
416 stimulates food intake (Zhou et al., 2013), may indicate that the changes leading to anorexia in fish
417 suffering enteromyxosis (Sitjà-Bobadilla and Palenzuela, 2012) are induced early in the infection.
418 The down-regulation of other genes acting in the digestive process, although not numerous, also
419 points towards diminished feeding activity and, in this sense, the up-regulation of *GCG2* may
420 reflect the effort in maintaining euglycemia. Finally, *VIP* product also has been recognized as an
421 immunomodulatory peptide with immunosuppressive function (Delgado et al., 2004), so its reduced

422 expression may be due to the immune defence response, as previously suggested (Bermúdez et al.,
423 2007).

424

425 3.9. Conclusions

426 The pathogenesis of enteromyxosis still has many unknown features, especially those related
427 to the incipient phase of infection. The parasite in the pre-patent period circumvents the host
428 response and successfully reaches and penetrates the intestinal lining epithelium. The findings of
429 this work constitute a basis for deciphering the mechanisms acting during this phase. A schematic
430 diagram summarizing the main results is presented in Fig. 6. The turbot immune response during
431 early enteromyxosis is chiefly characterized by signalling pathways involving IFNs, in contrast to
432 that observed in advanced infection, and only some mechanisms of innate immunity are shared
433 between both stages. There is some evidence of possible targets for parasite immune system evasion
434 such as complement components and APP, which possibly hinder a proper acute phase response. At
435 an intestinal level, the invasion and colonization strategies of *E. scophthalmi* appear to involve
436 cytoskeleton remodelling of the host cells and inhibition of epithelial renewal. Also, it is noteworthy
437 that one of the fish analyzed, which presented more mature and spreading stages of the myxozoan,
438 showed less intense transcriptomic changes. Further studies using more individuals or families are
439 required to ascertain the consistency and causes of this observation, although it suggests a silencing
440 of the host response, which would allow the early proliferation and colonization of vast areas of the
441 gastrointestinal lining epithelium by *E. scophthalmi*. Likely, when the parasite load and the related
442 tissue damage become important, the immune response is triggered. However, as pointed out by
443 different studies, this delayed response, which is exacerbated at a local level contributing to the
444 severe intestinal lesions, is ineffective. The transcriptomic analysis performed here has brought
445 novel and intriguing information about host-parasite interactions in enteromyxosis. The

446 identification of the molecular actors and their roles may speed the development of early detection,
447 control and therapeutic strategies, and even to identify targets for breeding programs.

448

449 **Acknowledgements**

450 The authors would like to thank María José Redondo and María E. Alonso-Naveiro for the
451 assistance with the infection trial. Also, we want to acknowledge Lucía Insua, María del Carmen
452 Carreira and Sandra Maceiras for technical assistance. This study was funded by the Spanish
453 Ministry of Economy and Competitiveness (AGL 2009-13282-C02-01 and -02; AGL2015-67039-
454 C3-1-R and AGL2015-67039-C3-3-R), the European Regional Development's funds (FEDER) and
455 Xunta de Galicia (Spain) local government (GRC2014/010 and GPC2015/34). Diego Robledo was
456 supported by a FPU fellowship funded by the Spanish Ministry of Education, Culture and Sport.
457 Paolo Ronza was supported by a grant from the scientific network “INMUNOGENOM”, funded by
458 Xunta de Galicia (REDES GI-1251). We acknowledge the support of the Centro de
459 Supercomputación de Galicia (CESGA), Spain, in the completion of this work.

460

461 **References**

- 462 Armstrong, P.B., 2006. Proteases and protease inhibitors: a balance of activities in host-pathogen
463 interaction. *Immunobiology* 211, 263-281.
- 464 APROMAR, 2015. La Acuicultura en España 2015. Available online at
465 <http://www.apromar.es/content/informes-anuales>
- 466 Bayne, C.J., Gerwick, L., 2001. The acute phase response and innate immunity of fish. *Dev Comp*
467 *Immunol* 25, 725-743.
- 468 Beiting, D.P., 2014. Protozoan parasites and type I interferons: a cold case reopened. *Trends*
469 *Parasitol* 30, 491-498.
- 470 Ben-Othman, R., Flannery, A.R., Miguel, D.C., Ward, D.M., Kaplan, J., Andrews, N.W., 2014.
471 *Leishmania*-mediated inhibition of iron export promotes parasite replication in
472 macrophages. *PLoS Pathog* 10, e1003901.
- 473 Bermúdez, R., Losada, A.P., Vázquez, S., Redondo, M.J., Álvarez-Pellitero, P., Quiroga, M.I.,
474 2010. Light and electron microscopic studies on turbot *Psetta maxima* infected with
475 *Enteromyxum scophthalmi*: histopathology of turbot enteromyxosis. *Dis Aquat Organ* 89,
476 209-221.
- 477 Bermúdez, R., Vigliano, F., Marcaccini, A., Sitjà-Bobadilla, A., Quiroga, M.I., Nieto, J.M., 2006.
478 Response of Ig-positive cells to *Enteromyxum scophthalmi* (Myxozoa) experimental
479 infection in turbot, *Scophthalmus maximus* (L.): A histopathological and
480 immunohistochemical study. *Fish Shellfish Immunol* 21, 501-512.
- 481 Bermúdez, R., Vigliano, F., Quiroga, M.I., Nieto, J.M., Bosi, G., Domeneghini, C., 2007.
482 Immunohistochemical study on the neuroendocrine system of the digestive tract of turbot,
483 *Scophthalmus maximus* (L.), infected by *Enteromyxum scophthalmi* (Myxozoa). *Fish*
484 *Shellfish Immunol* 22, 252-263.

- 485 Bimal, S., Singh, S.K., Sinha, S., Pandey, K., Sinha, P.K., Ranjan, A., Bhattacharya, S.K., Das, P.,
486 2008. *Leishmania donovani*: role of CD2 on CD4+ T-cell function in Visceral
487 Leishmaniasis. *Exp Parasitol* 118, 238-246.
- 488 Bjork, S.J., Zhang, Y.A., Hurst, C.N., Alonso-Naveiro, M.E., Alexander, J.D., Sunyer, J.O.,
489 Bartholomew, J.L., 2014. Defenses of susceptible and resistant Chinook salmon
490 (*Oncorhynchus tshawytscha*) against the myxozoan parasite *Ceratomyxa shasta*. *Fish*
491 *Shellfish Immunol* 37, 87-95.
- 492 Bolger, A.M., Lohse, M., Usadel, B., 2014. Trimmomatic: a flexible trimmer for Illumina sequence
493 data. *Bioinformatics* 30, 2114-2120.
- 494 Castanier, C., Garcin, D., Vazquez, A., Arnoult, D., 2010. Mitochondrial dynamics regulate the
495 RIG-I-like receptor antiviral pathway. *EMBO Rep* 11, 133-138.
- 496 Cliffe, L.J., Humphreys, N.E., Lane, T.E., Potten, C.S., Booth, C., Grecis, R.K., 2005. Accelerated
497 intestinal epithelial cell turnover: a new mechanism of parasite expulsion. *Science* 308,
498 1463-1465.
- 499 Conesa, A., Gotz, S., Garcia-Gomez, J.M., Terol, J., Talon, M., Robles, M., 2005. Blast2GO: a
500 universal tool for annotation, visualization and analysis in functional genomics research.
501 *Bioinformatics* 21, 3674-3676.
- 502 Cortes, A., Munoz-Antoli, C., Martin-Grau, C., Esteban, J.G., Grecis, R.K., Toledo, R., 2015.
503 Differential alterations in the small intestine epithelial cell turnover during acute and chronic
504 infection with *Echinostoma caproni* (Trematoda). *Parasit Vectors* 8, 334.
- 505 Costa, V., Aprile, M., Esposito, R., Ciccodicola, A., 2013. RNA-Seq and human complex diseases:
506 recent accomplishments and future perspectives. *Eur J Hum Genet* 21, 134-142.
- 507 Chen, X.M., Huang, B.Q., Splinter, P.L., Orth, J.D., Billadeau, D.D., McNiven, M.A., LaRusso,
508 N.F., 2004. Cdc42 and the actin-related protein/neural Wiskott-Aldrich syndrome protein

- 509 network mediate cellular invasion by *Cryptosporidium parvum*. Infect Immun 72, 3011-
510 3021.
- 511 Davey, G.C., Calduch-Giner, J.A., Houeix, B., Talbot, A., Sitjà-Bobadilla, A., Prunet, P., Pérez-
512 Sánchez, J., Cairns, M.T., 2011. Molecular profiling of the gilthead sea bream (*Sparus*
513 *aurata* L.) response to chronic exposure to the myxosporean parasite *Enteromyxum leei*. Mol
514 Immunol 48, 2102-2112.
- 515 Delgado, M., Pozo, D., Ganea, D., 2004. The significance of vasoactive intestinal peptide in
516 immunomodulation. Pharmacol Rev 56, 249-290.
- 517 Dixit, E., Kagan, J.C., 2013. Intracellular pathogen detection by RIG-I-like receptors. Adv Immunol
518 117, 99-125.
- 519 Estensoro, I., Redondo, M.J., Álvarez-Pellitero, P., Sitjà-Bobadilla, A., 2014. Immunohistochemical
520 characterization of polyclonal antibodies against *Enteromyxum leei* and *Enteromyxum*
521 *scophthalmi* (Myxozoa: Myxosporidia), intestinal parasites of fish. J Fish Dis 37, 785-796.
- 522 Figueras, A., Robledo, D., Corvelo, A., Hermida, M., Pereiro, P., Rubiolo, J.A., Gómez-Garrido, J.,
523 Carreté L., Bello, X., Gut, M., Gut, I.G., Marcet-Houben, M., Forn-Cuní, G., Abal-Fabeiro,
524 J.L., Pardo, B.G., Taboada, X., Fernández, C., Vlasova, A., Hermoso-Pulido, A., Guigó, R.,
525 Álvarez-Dios, J.A., Gómez-Tato, A., Viñas, A., Maside, X., Gabaldón, T., Novoa, B.,
526 Bouza, C., Alioto, T., Martínez, P., 2016. Whole genome sequencing of turbot
527 (*Scophthalmus maximus*; Pleuronectiformes): a fish adapted to demersal life. DNA Res, in
528 press, doi: 10.1093/dnares/dsw007.
- 529 Gerwick, L., Steinhauer, R., Lapatra, S., Sandell, T., Ortuno, J., Hajiseyedjavadi, N., Bayne, C.J.,
530 2002. The acute phase response of rainbow trout (*Oncorhynchus mykiss*) plasma proteins to
531 viral, bacterial and fungal inflammatory agents. Fish Shellfish Immunol 12, 229-242.

- 532 Gruenheid, S., Finlay, B.B., 2003. Microbial pathogenesis and cytoskeletal function. *Nature* 422,
533 775-781.
- 534 Iwai, H., Kim, M., Yoshikawa, Y., Ashida, H., Ogawa, M., Fujita, Y., Muller, D., Kirikae, T.,
535 Jackson, P.K., Kotani, S., Sasakawa, C., 2007. A bacterial effector targets Mad2L2, an APC
536 inhibitor, to modulate host cell cycling. *Cell* 130, 611-623.
- 537 Kanehisa, M., Sato, Y., Kawashima, M., Furumichi, M., Tanabe, M., 2016. KEGG as a reference
538 resource for gene and protein annotation. *Nucleic Acids Res* 44, D457-462.
- 539 Kashiwada, M., Cassel, S.L., Colgan, J.D., Rothman, P.B., 2011. NFIL3/E4BP4 controls type 2 T
540 helper cell cytokine expression. *EMBO J* 30, 2071-2082.
- 541 Kautz, L., Jung, G., Valore, E.V., Rivella, S., Nemeth, E., Ganz, T., 2014. Identification of
542 erythroferrone as an erythroid regulator of iron metabolism. *Nat Genet* 46, 678-684.
- 543 Khoo, C.-K., Abdul-Murad, A.M., Kua, B.-C., Mohd-Adnan, A., 2012. *Cryptocaryon irritans*
544 infection induces the acute phase response in *Lates calcarifer*: A transcriptomic perspective.
545 *Fish Shellfish Immunol* 33, 788-794.
- 546 Kim, D., Pertea, G., Trapnell, C., Pimentel, H., Kelley, R., Salzberg, S.L., 2013. TopHat2: accurate
547 alignment of transcriptomes in the presence of insertions, deletions and gene fusions.
548 *Genome Biol* 14, R36.
- 549 Kim, M., Ogawa, M., Mimuro, H., Sasakawa, C., 2010. Reinforcement of epithelial cell adhesion to
550 basement membrane by a bacterial pathogen as a new infectious stratagem. *Virulence* 1, 52-
551 55.
- 552 Kim, Y.E., Ahn, J.H., 2015. Positive role of promyelocytic leukemia protein in type I interferon
553 response and its regulation by human cytomegalovirus. *PLoS Pathog* 11, e1004785.
- 554 Koshiba, T., 2013. Mitochondrial-mediated antiviral immunity. *Biochim Biophys Acta* 1833, 225-
555 232.

- 556 Kovacevic, N., Hagen, M.O., Xie, J., Belosevic, M., 2015. The analysis of the acute phase response
557 during the course of *Trypanosoma carassii* infection in the goldfish (*Carassius auratus* L.).
558 Dev Comp Immunol 53, 112-122.
- 559 Langmead, B., Salzberg, S.L., 2012. Fast gapped-read alignment with Bowtie 2. Nat Methods 9,
560 357-359.
- 561 Leon-Sicairos, N., Reyes-Cortes, R., Guadrón-Llanos, A.M., Madueña-Molina, J., Leon-Sicairos,
562 C., Canizalez-Román, A., 2015. Strategies of intracellular pathogens for obtaining iron from
563 the environment. Biomed Res Int 2015, 17.
- 564 Li, C., Beck, B., Su, B., Terhune, J., Peatman, E., 2013. Early mucosal responses in blue catfish
565 (*Ictalurus furcatus*) skin to *Aeromonas hydrophila* infection. Fish Shellfish Immunol 34,
566 920-928.
- 567 Li, C., Zhang, Y., Wang, R., Lu, J., Nandi, S., Mohanty, S., Terhune, J., Liu, Z., Peatman, E., 2012.
568 RNA-seq analysis of mucosal immune responses reveals signatures of intestinal barrier
569 disruption and pathogen entry following *Edwardsiella ictaluri* infection in channel catfish,
570 *Ictalurus punctatus*. Fish Shellfish Immunol 32, 816-827.
- 571 Li, B., Dewey, C.N., 2011. RSEM: accurate transcript quantification from RNA-seq data with or
572 without a reference genome. BMC Bioinformatics 12, 323.
- 573 Li, Q., Freeman, L.M., Rush, J.E., Huggins, G.S., Kennedy, A.D., Labuda, J.A., Laflamme, D.P.,
574 Hannah, S.S., 2015. Veterinary medicine and multi-omics research for future nutrition
575 targets: metabolomics and transcriptomics of the common degenerative mitral valve disease
576 in dogs. OMICS 19, 461-470.
- 577 Liu, J., Deng, M., Lancto, C.A., Abrahamsen, M.S., Rutherford, M.S., Enomoto, S., 2009. Biphasic
578 modulation of apoptotic pathways in *Cryptosporidium parvum*-infected human intestinal
579 epithelial cells. Infect Immun 77, 837-849.

- 580 Lodge, R., Descoteaux, A., 2006. Phagocytosis of *Leishmania donovani* amastigotes is Rac1
581 dependent and occurs in the absence of NADPH oxidase activation. Eur J Immunol 36,
582 2735-2744.
- 583 Losada, A.P., Bermúdez, R., Faílde, L.D., de Ocenda, M.V.R., Quiroga, M.I., 2014a. Study of the
584 distribution of active caspase-3-positive cells in turbot, *Scophthalmus maximus* (L.),
585 enteromyxosis. J Fish Dis 37, 21-32.
- 586 Losada, A.P., Bermúdez, R., Faílde, L.D., Di Giancamillo, A., Domeneghini, C., Quiroga, M.I.,
587 2014b. Effects of *Enteromyxum scophthalmi* experimental infection on the neuroendocrine
588 system of turbot, *Scophthalmus maximus* (L.). Fish Shellfish Immunol 40, 577-583.
- 589 Losada, A.P., Bermúdez, R., Faílde, L.D., Quiroga, M.I., 2012. Quantitative and qualitative
590 evaluation of iNOS expression in turbot (*Psetta maxima*) infected with *Enteromyxum*
591 *scophthalmi*. Fish Shellfish Immunol 32, 243-248.
- 592 Luo, M., Sainsbury, J., Tuff, J., Lacap, P.A., Yuan, X.Y., Hirbod, T., Kimani, J., Wachihi, C.,
593 Ramdahin, S., Bielawny, T., Embree, J., Broliden, K., Ball, T.B., Plummer, F.A., 2012. A
594 genetic polymorphism of FREM1 is associated with resistance against HIV infection in the
595 Pumwani sex worker cohort. J Virol 86, 11899-11905.
- 596 Manocha, G.D., Mishra, R., Sharma, N., Kumawat, K.L., Basu, A., Singh, S.K., 2014. Regulatory
597 role of TRIM21 in the type-I interferon pathway in Japanese encephalitis virus-infected
598 human microglial cells. J Neuroinflammation 11, 24.
- 599 McEwan, W.A., Tam, J.C.H., Watkinson, R.E., Bidgood, S.R., Mallery, D.L., James, L.C., 2013.
600 Intracellular antibody-bound pathogens stimulate immune signaling via the Fc receptor
601 TRIM21. Nat Immunol 14, 327-336.
- 602 McGavin, D., Zachary, J.F., 2006. Pathologic Basis of Veterinary Disease. Elsevier Health
603 Sciences, New York, NY, USA.

- 604 Melo, M.B., Nguyen, Q.P., Cordeiro, C., Hassan, M.A., Yang, N., McKell, R., Rosowski, E.E.,
605 Julien, L., Butty, V., Darde, M.L., Ajzenberg, D., Fitzgerald, K., Young, L.H., Saeij, J.P.,
606 2013. Transcriptional analysis of murine macrophages infected with different *Toxoplasma*
607 strains identifies novel regulation of host signaling pathways. PLoS Pathog 9, e1003779.
- 608 Mimuro, H., Suzuki, T., Nagai, S., Rieder, G., Suzuki, M., Nagai, T., Fujita, Y., Nagamatsu, K.,
609 Ishijima, N., Koyasu, S., Haas, R., Sasakawa, C., 2007. *Helicobacter pylori* dampens gut
610 epithelial self-renewal by inhibiting apoptosis, a bacterial strategy to enhance colonization
611 of the stomach. Cell Host Microbe 2, 250-263.
- 612 Mittal, K., Welter, B.H., Temesvari, L.A., 2008. *Entamoeba histolytica*: lipid rafts are involved in
613 adhesion of trophozoites to host extracellular matrix components. Exp Parasitol 120, 127-
614 134.
- 615 Moon, T.W., 1998. Glucagon: from hepatic binding to metabolism in teleost fish. Comp Biochem
616 Phys B 121, 27-34.
- 617 Nde, P.N., Lima, M.F., Johnson, C.A., Pratap, S., Villalta, F., 2012. Regulation and use of the
618 extracellular matrix by *Trypanosoma cruzi* during early infection. Front Immunol 3, 337.
- 619 Nie, L., Xiong, R., Zhang, Y.S., Zhu, L.Y., Shao, J.Z., Xiang, L.X., 2014. Conserved inhibitory role
620 of teleost SOCS-1s in IFN signaling pathways. Dev Comp Immunol 43, 23-29.
- 621 Onoguchi, K., Onomoto, K., Takamatsu, S., Jogi, M., Takemura, A., Morimoto, S., Julkunen, I.,
622 Namiki, H., Yoneyama, M., Fujita, T., 2010. Virus-infection or 5'ppp-RNA activates
623 antiviral signal through redistribution of IPS-1 mediated by MFN1. PLoS Pathog 6,
624 e1001012.
- 625 Peatman, E., Baoprasertkul, P., Terhune, J., Xu, P., Nandi, S., Kucuktas, H., Li, P., Wang, S.,
626 Somridhivej, B., Dunham, R., Liu, Z., 2007. Expression analysis of the acute phase response

- 627 in channel catfish (*Ictalurus punctatus*) after infection with a Gram-negative bacterium. Dev
628 Comp Immunol 31, 1183-1196.
- 629 Pereiro, P., Figueras, A., Novoa, B., 2012. A novel hepcidin-like in turbot (*Scophthalmus maximus*
630 L.) highly expressed after pathogen challenge but not after iron overload. Fish Shellfish
631 Immunol 32, 879-889.
- 632 Peterson, L.W., Artis, D., 2014. Intestinal epithelial cells: regulators of barrier function and immune
633 homeostasis. Nat Rev Immunol 14, 141-153.
- 634 Qian, X., Ba, Y., Zhuang, Q., Zhong, G., 2014. RNA-Seq technology and its application in fish
635 transcriptomics. OMICS 18, 98-110.
- 636 Quiroga, M.I., Redondo, M.J., Sitjà-Bobadilla, A., Palenzuela, O., Riaza, A., Macías, A., Vázquez,
637 S., Pérez, A., Nieto, J.M., Álvarez-Pellitero, P., 2006. Risk factors associated with
638 *Enteromyxum scophthalmi* (Myxozoa) infection in cultured turbot, *Scophthalmus maximus*
639 (L.). Parasitology 133, 433-442.
- 640 Radhakrishnan, G.K., Splitter, G.A., 2012. Modulation of host microtubule dynamics by pathogenic
641 bacteria. Biomol Concepts 3, 571-580.
- 642 Redondo, M.J., Álvarez-Pellitero, P., 2010. The effect of lectins on the attachment and invasion of
643 *Enteromyxum scophthalmi* (Myxozoa) in turbot (*Psetta maxima* L.) intestinal epithelium in
644 vitro. Exp Parasitol 126, 577-581.
- 645 Redondo, M.J., Palenzuela, O., Álvarez-Pellitero, P., 2004. Studies on transmission and life cycle of
646 *Enteromyxum scophthalmi* (Myxozoa), an enteric parasite of turbot *Scophthalmus maximus*.
647 Folia Parasitol (Praha) 51, 188-198.
- 648 Redondo, M.J., Palenzuela, O., Riaza, A., Macías, A., Álvarez-Pellitero, P., 2002. Experimental
649 transmission of *Enteromyxum scophthalmi* (Myxozoa), an enteric parasite of turbot
650 *Scophthalmus maximus*. J Parasitol 88, 482-488.

- 651 Redondo, M.J., Quiroga, M.I., Palenzuela, O., Nieto, J.M., Álvarez-Pellitero, P., 2003.
652 Ultrastructural studies on the development of *Enteromyxum scophthalmi* (Myxozoa), an
653 enteric parasite of turbot (*Scophthalmus maximus* L.). Parasitol Res 90, 192-202.
- 654 Robinson, M.D., Oshlack, A., 2010. A scaling normalization method for differential expression
655 analysis of RNA-seq data. Genome Biol 11, R25.
- 656 Robledo, D., Ronza, P., Harrison, P.W., Losada, A.P., Bermúdez, R., Pardo, B.G., Redondo, M.J.,
657 Sitjà-Bobadilla, A., Quiroga, M.I., Martínez, P., 2014. RNA-seq analysis reveals significant
658 transcriptome changes in turbot (*Scophthalmus maximus*) suffering severe enteromyxosis.
659 BMC Genomics 15, 1149.
- 660 Simpson, J.T., Wong, K., Jackman, S.D., Schein, J.E., Jones, S.J.M., Birol, I., 2009. ABySS: A
661 parallel assembler for short read sequence data. Genome Res 19, 1117-1123.
- 662 Singh, B., Fleury, C., Jalalvand, F., Riesbeck, K., 2012. Human pathogens utilize host extracellular
663 matrix proteins laminin and collagen for adhesion and invasion of the host. FEMS Microbiol
664 Rev 36, 1122-1180.
- 665 Sitjà-Bobadilla, A., Palenzuela, O., 2012. *Enteromyxum* Species, in: Woo, P.T.K., Buchmann, K.
666 (Eds.), Fish Parasites: Pathobiology and Protection. CABI publishing, UK, pp. 163-176.
- 667 Sitjà-Bobadilla, A., Redondo, M.J., Bermúdez, R., Palenzuela, O., Ferreiro, I., Riaza, A., Quiroga,
668 I., Nieto, J.M., Álvarez-Pellitero, P., 2006. Innate and adaptive immune responses of turbot,
669 *Scophthalmus maximus* (L.), following experimental infection with *Enteromyxum*
670 *scophthalmi* (Myxosporidia: Myxozoa). Fish Shellfish Immunol 21, 485-500.
- 671 Sun, F., Peatman, E., Li, C., Liu, S., Jiang, Y., Zhou, Z., Liu, Z., 2012. Transcriptomic signatures of
672 attachment, NF-kappaB suppression and IFN stimulation in the catfish gill following
673 columnaris bacterial infection. Dev Comp Immunol 38, 169-180.

- 674 Suzuki, T., 2013. Regulation of intestinal epithelial permeability by tight junctions. *Cell Mol Life*
675 *Sci* 70, 631-659.
- 676 Tran, D.Q., Andersson, J., Wang, R., Ramsey, H., Unutmaz, D., Shevach, E.M., 2009. GARP
677 (LRRC32) is essential for the surface expression of latent TGF-beta on platelets and
678 activated FOXP3+ regulatory T cells. *Proc Natl Acad Sci U S A* 106, 13445-13450.
- 679 Vaysburd, M., Watkinson, R.E., Cooper, H., Reed, M., O'Connell, K., Smith, J., Cruickshanks, J.,
680 James, L.C., 2013. Intracellular antibody receptor TRIM21 prevents fatal viral infection.
681 *Proc Natl Acad Sci U S A* 110, 12397-12401.
- 682 Wu, J., Mao, X., Cai, T., Luo, J., Wei, L., 2006. KOBAS server: a web-based platform for
683 automated annotation and pathway identification. *Nucleic Acids Res* 34, W720-W724.
- 684 Xu, J.H., Qin, Z.H., Liao, Y.S., Xie, M.Q., Li, A.X., Cai, J.P., 2008. Characterization and
685 expression of an actin-depolymerizing factor from *Eimeria tenella*. *Parasitol Res* 103, 263-
686 270.
- 687 Young, N.D., Cooper, G.A., Nowak, B.F., Koop, B.F., Morrison, R.N., 2008. Coordinated down-
688 regulation of the antigen processing machinery in the gills of amoebic gill disease-affected
689 Atlantic salmon (*Salmo salar* L.). *Mol Immunol* 45, 2581-2597.
- 690 Zhang, J., Yu, L.P., Li, M.F., Sun, L., 2014. Turbot (*Scophthalmus maximus*) hepcidin-1 and
691 hepcidin-2 possess antimicrobial activity and promote resistance against bacterial and viral
692 infection. *Fish Shellfish Immunol* 38, 127-134.
- 693 Zhang, W., Zhang, J., Kornuc, M., Kwan, K., Frank, R., Nimer, S.D., 1995. Molecular cloning and
694 characterization of NF-IL3A, a transcriptional activator of the human interleukin-3
695 promoter. *Mol Cell Biol* 15, 6055-6063.

- 696 Zhou, Y., Liang, X.-F., Yuan, X., Li, J., He, Y., Fang, L., Guo, X., Liu, L., Li, B., Shen, D., 2013.
 697 Neuropeptide Y stimulates food intake and regulates metabolism in grass carp,
 698 *Ctenopharyngodon idellus*. *Aquaculture* 380–383, 52-61.
- 699 Zipfel, P.F., Wurzner, R., Skerka, C., 2007. Complement evasion of pathogens: common strategies
 700 are shared by diverse organisms. *Mol Immunol* 44, 3850-3857.
- 701 Zou, J., Secombes, C.J., 2011. Teleost fish interferons and their role in immunity. *Dev Comp*
 702 *Immunol* 35, 1376-1387.

703 **TABLES**

704 **Table 1.** Comparison between genome-guided and de novo transcriptome assemblies from RNA-seq data
 705 obtained from samples of control and *Enteromyxum scophthalmi*-infected turbot (*Scophthalmus maximus*).

	Genome-guided	De novo
Number of reads	160 million	-
Reads mapped to the genome	138 million	-
Reads for de novo assembly	-	18 million ^a
Total transcripts	56,321	328,480
N50 ^b	5073	1510

706 ^a Total unaligned reads from pyloric caeca samples at 24 and 42 days post-inoculation.

707 ^bN50 is the length for which the collection of all transcripts of that length or longer contains at least half of
 708 the sum of the lengths of all transcripts.

709

710 **FIGURE LEGENDS**

711 **Fig. 1.** Histopathology (A, B, D, E; stained with toluidine blue) and immunohistochemistry (C, F)
 712 of pyloric caeca from turbot (*Scophthalmus maximus*) infected by *Enteromyxum scophthalmi*. (A)
 713 Note the slight inflammatory infiltration at the basal part of the lining epithelium (arrowhead) and
 714 in the lamina propria-submucosa (asterisk). Also, round basophilic structures can be seen in the
 715 epithelial lining of an intestinal fold (black arrows). Scale bar = 100 µm. (B) Higher magnification
 716 of pyloric caeca showing the infiltration of mononuclear cells in the basal part of the epithelium
 717 (arrowhead) and the lamina propria-submucosa (black arrow). Note the round basophilic structures

718 near the basement membrane of the epithelial lining (white arrow), consistent with early
719 development stages of *E. scophthalmi*. Scale bar = 50 μ m. (C) Immunohistochemical detection of
720 two early stages of *E. scophthalmi* (brown colored) in the basal part of the epithelium. Scale bar =
721 20 μ m. (D - F) Histological section from the pyloric caeca of the infected turbot 2. (D) Note the
722 presence of two parasitic structures in the epithelial lining, associated with a very mild
723 inflammatory infiltration. Scale bar = 100 μ m. (E) Higher magnification showing a trophozoite
724 (arrowhead), consistent with a developmental stage 3 of *E. scophthalmi*. Scale bar = 50 μ m. (F)
725 Immunostaining of a parasitic structure with the polyclonal antibody against *E. scophthalmi*. Scale
726 bar = 20 μ m.

727

728 **Fig. 2.** Hierarchical clustering of samples by organ from turbot (*Scophthalmus maximus*) at 24 days
729 post-inoculation with *Enteromyxum scophthalmi*. Hierarchical clustering of all infected (-1, -2, -3)
730 and control (Ctrl) samples for (A) head kidney, (B) spleen and (C) pyloric caeca. Approximate
731 unbiased *P* values, computed by multi-scale bootstrap resampling, are displayed on branch nodes.

732

733 **Fig. 3.** Heatmaps of differentially expressed genes of interest in turbot (*Scophthalmus maximus*) at
734 24 days post-inoculation with *Enteromyxum scophthalmi*. Heatmaps for (A) head kidney, (B) spleen
735 and (C) pyloric caeca showing the expression of several genes of interest, labelling their functional
736 category. Displayed are EdgeR (Robinson and Oshlack, 2010) normalized counts for each sample
737 and gene. Expression values for each gene have been scaled from -1 to 1 by subtracting the mean
738 and dividing by the standard deviation. Genes were hierarchically clustered according to their gene
739 expression using Pearson correlation as a distance measure. 1, 2, 3, infected turbot numbers 1, 2, 3;
740 C, control. Full names of genes are shown in Supplementary Tables S2 - S4.

741

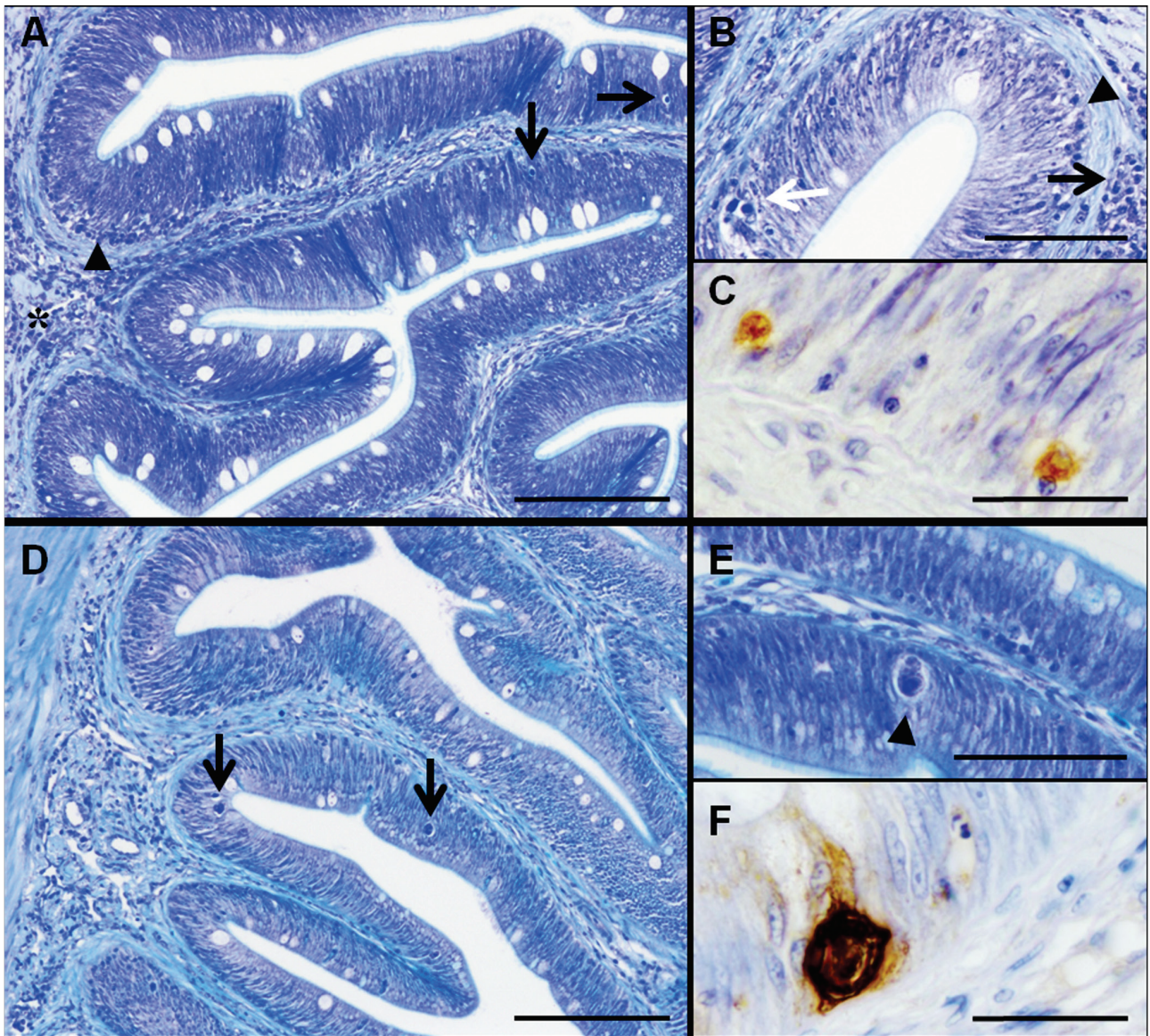
742 **Fig. 4.** Gene Ontology (GO) term enrichment among the differentially expressed genes for (A) head
743 kidney, (B) spleen and (C) pyloric caeca from turbot (*Scophthalmus maximus*) at 24 days post-
744 inoculation with *Enteromyxum scophthalmi*.

745

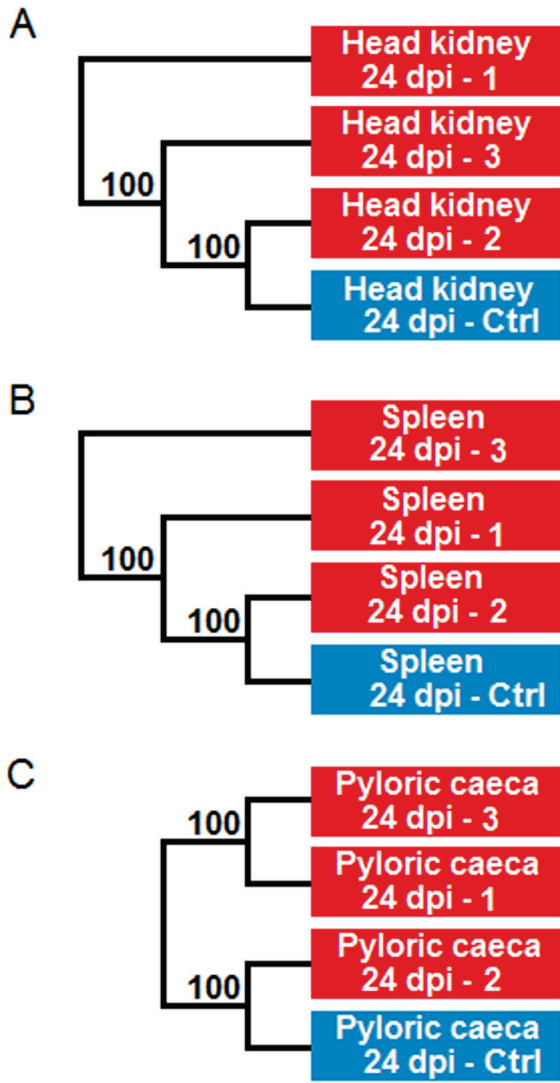
746 **Fig. 5.** Venn diagrams showing differentially expressed genes in (A) head kidney, (B) spleen and
747 (C) pyloric caeca from slightly (24d) and severely (42d) infected turbot (*Scophthalmus maximus*),
748 corresponding to 24 and 42 days post-inoculation with *Enteromyxum scophthalmi*.

749

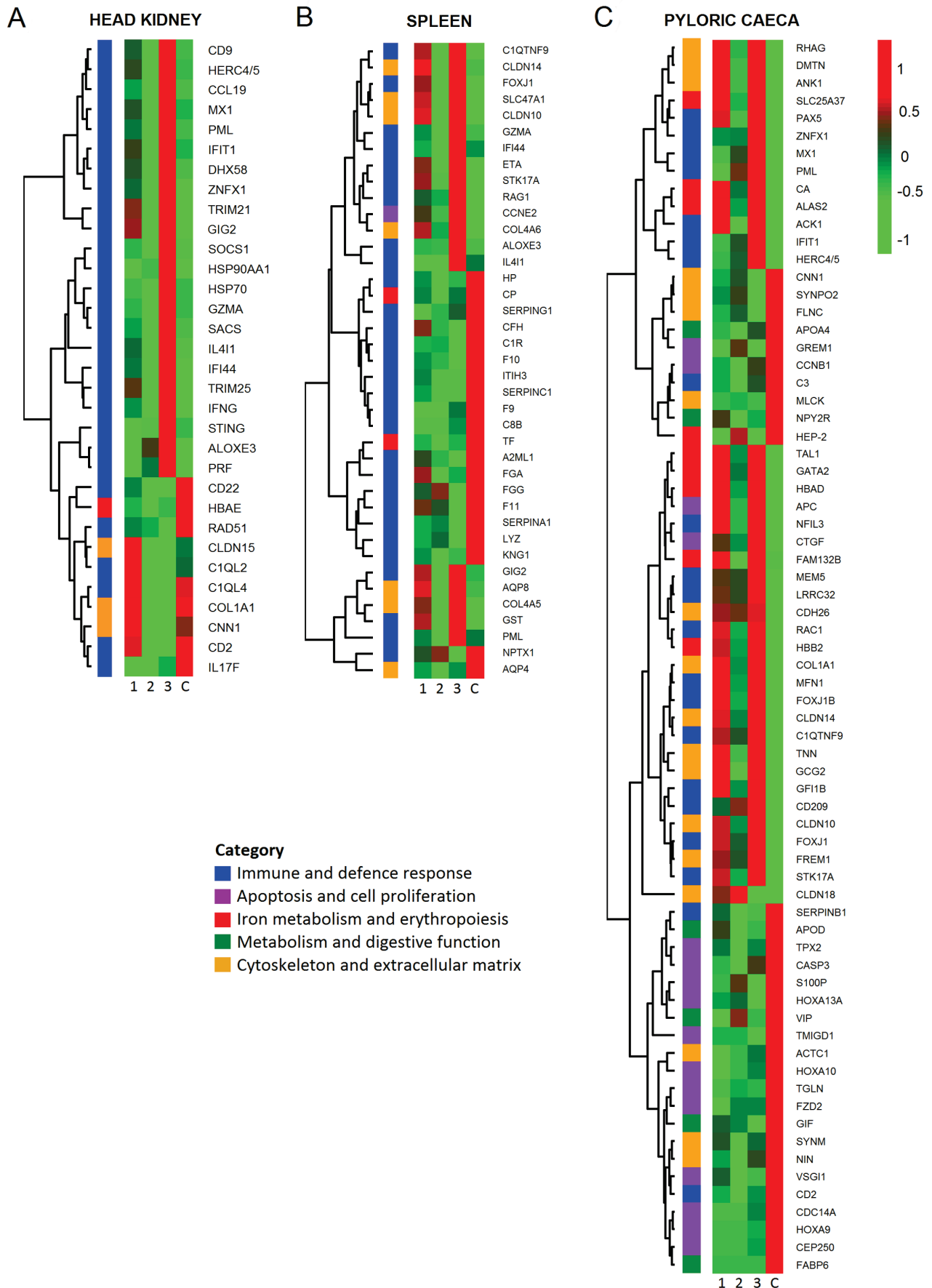
750 **Fig. 6.** Schematic diagram showing the main events involved in early enteromyxosis in turbot
751 (*Scophthalmus maximus*) inferred from the results of this study. ECM, extra-cellular matrix.



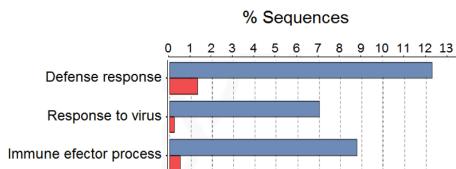
752



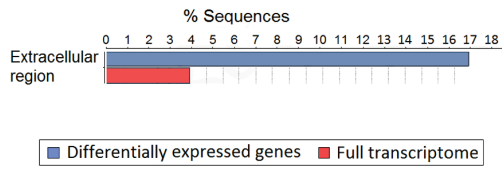
753



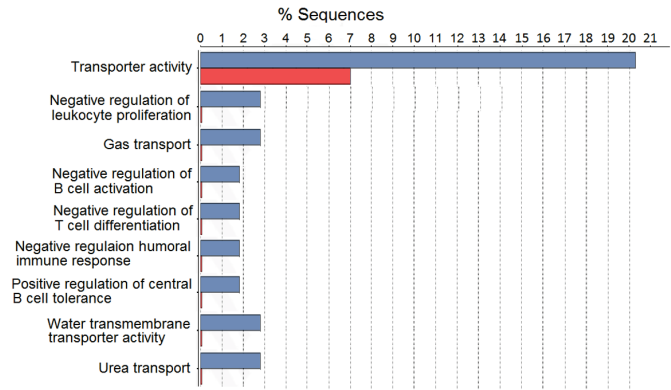
A HEAD KIDNEY



B SPLEEN



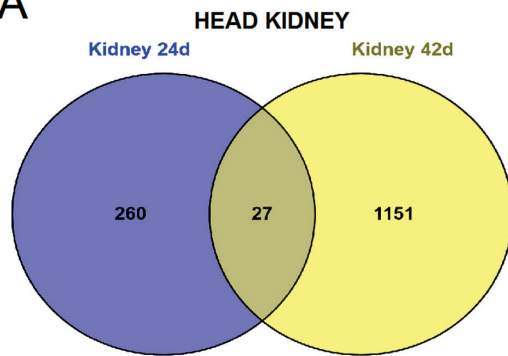
C PYLORIC CAECA



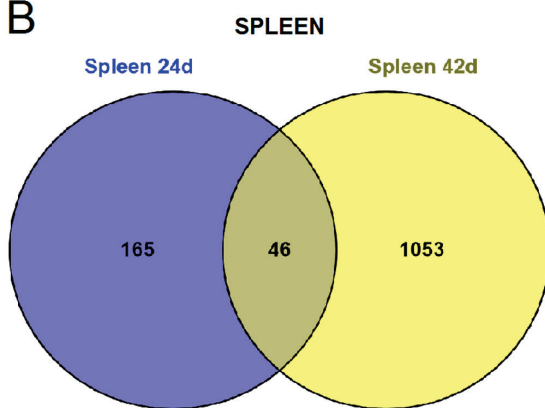
755

756

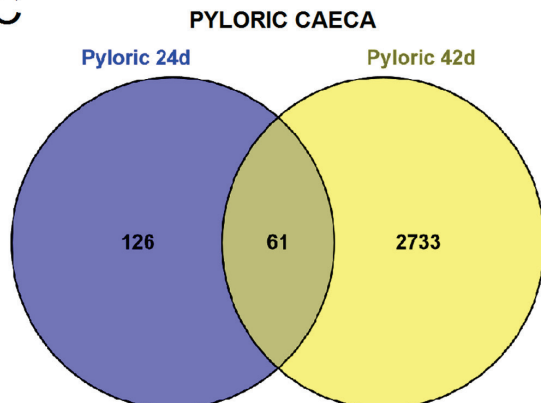
A



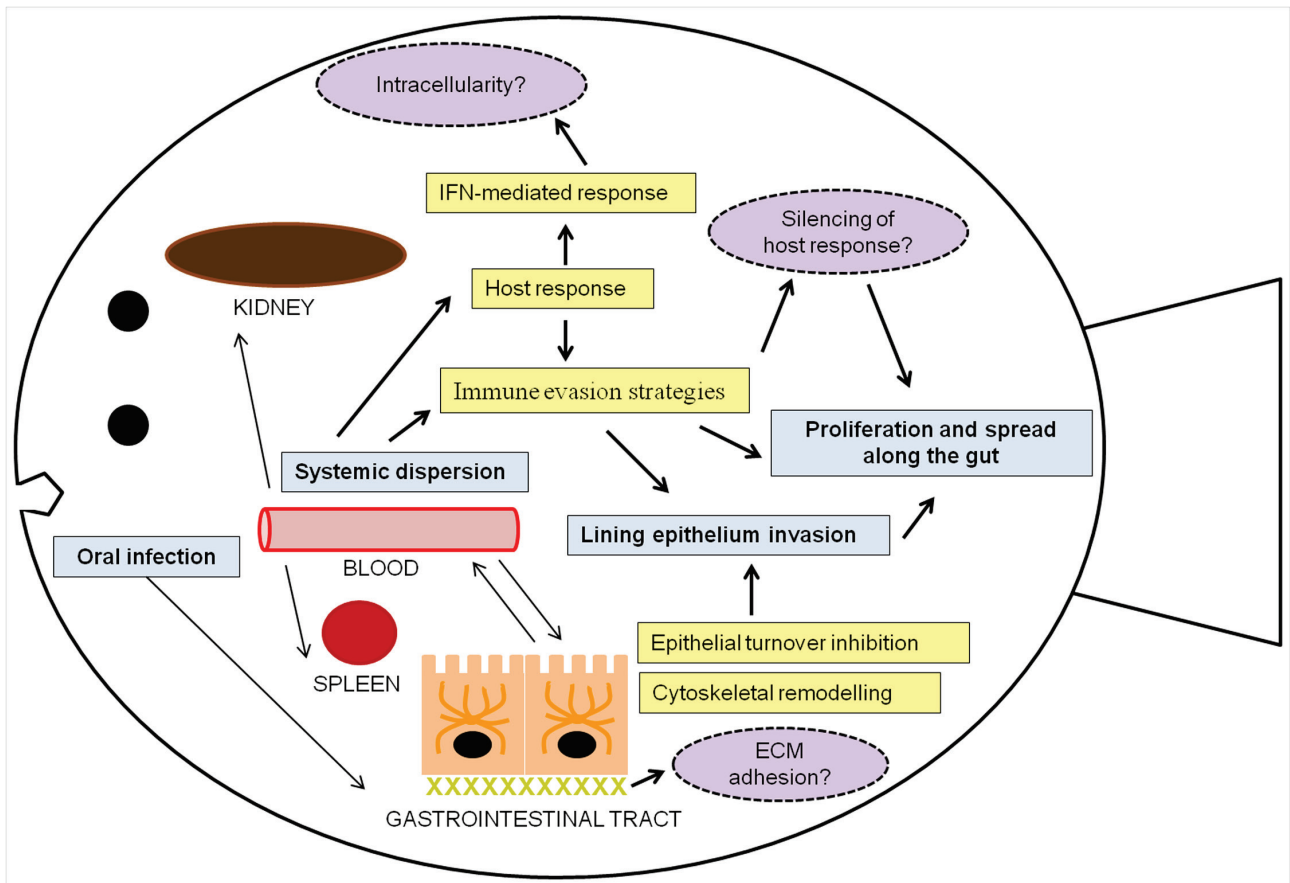
B



C



757



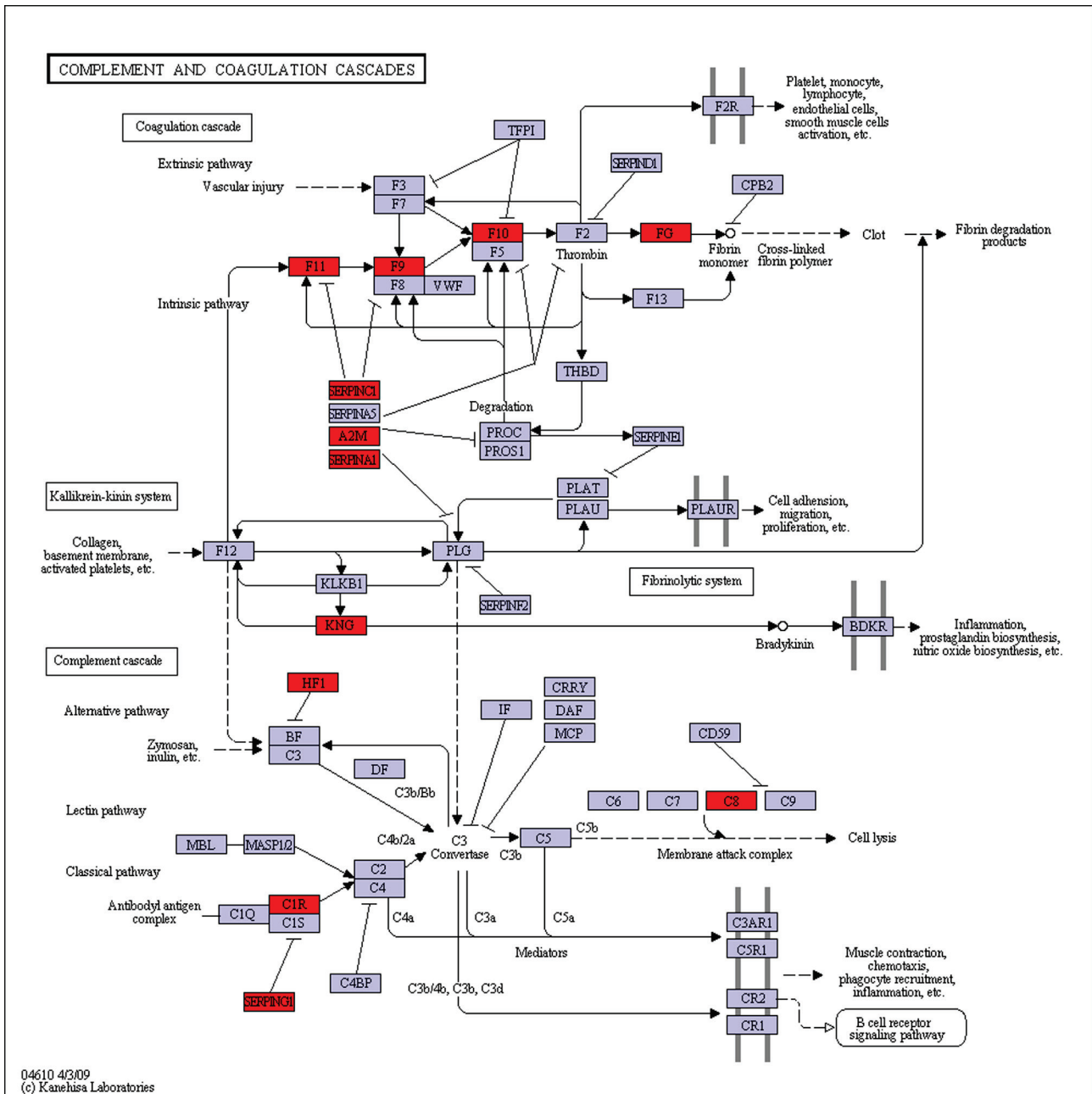
758

759

760 **SUPPLEMENTARY FIGURE LEGEND**

761

762 **Supplementary Fig. S1.** Illustration of the Kyoto Encyclopedia of Genes and Genomes (KEGG)
 763 pathway “complement and coagulation cascades”, which was statistically enriched (false discovery
 764 rate (FDR) corrected P value < 0.05) among the differentially expressed (DE) genes in the spleen of
 765 *Enteromyxum scophthalmi*-infected turbot (*Scophthalmus maximus*). The genes belonging to this
 766 pathway that were DE in the spleen of infected turbot are highlighted in red.



767

768

769 **SUPPLEMENTARY TABLES**

770 Supplementary tables S1 to S7 are available on the publisher Web site.